Cancer Research

Inhibition of Histone Lysine Methylation Enhances Cancer–Testis Antigen Expression in Lung Cancer Cells: Implications for Adoptive Immunotherapy of Cancer

Mahadev Rao[1], Nachimuthu Chinnasamy[2], Julie A. Hong[1], Yuwei Zhang[1], Mary Zhang[1], Sichuan Xi[1], Fang Liu[1], Victor E. Marquez[3], Richard A. Morgan[2], and David S. Schrump[1]

Abstract

Cancer–testis antigens (CTA), such as NY-ESO-1, MAGE-A1, and MAGE-A3, are immunogenic proteins encoded by genes, which are normally expressed only in male germ cells but are activated by ill-defined epigenetic mechanisms in human tumors, including lung cancers. Previously, we reported induction of these CTAs in cancer cells, but not normal cells, by DNA-demethylating agents and histone deacetylase inhibitors using clinically achievable exposure conditions. In the present study, we evaluated chromatin alterations associated with repression/activation of cancer–testis genes in lung cancer cells to further develop gene-induction regimens for cancer immunotherapy. Repression of *NY-ESO-1*, *MAGE-A1*, and *MAGE-A3* coincided with DNA hypermethylation, recruitment, and binding of polycomb-group proteins, and histone heterochromatin modifications within the promoters of these genes. Derepression coincided with DNA demethylation, dissociation of polycomb proteins, and presence of euchromatin marks within the respective promoters. Short hairpin RNAs were used to inhibit several histone methyltransferases (KMT) and histone demethylases (KDM) that mediate histone methylation and repress gene expression. Knockdown of KMT6, KDM1, or KDM5B markedly enhanced deoxyazacytidine (DAC)-mediated activation of these cancer–testis genes in lung cancer cells. DZNep, a pharmacologic inhibitor of KMT6 expression, recapitulated the effects of KMT6 knockdown. Following DAC–DZNep exposure, lung cancer cells were specifically recognized and lysed by allogeneic lymphocytes expressing recombinant T-cell receptors recognizing NY-ESO-1 and MAGE-A3. Combining DNA-demethylating agents with compounds, such as DZNep, that modulate histone lysine methylation may provide a novel epigenetic strategy to augment cancer–testis gene expression as an adjunct to adoptive cancer immunotherapy. *Cancer Res; 71(12); 4192–204. ©2011 AACR.*

Introduction

Cancer–testis antigens (CTA) are encoded by a unique class of genes [cancer–testis (CT) genes], normally expressed in germ cells or placenta, that are derepressed by epigenetic mechanisms in various human malignancies (1). Because they are typically expressed only in immune-privileged sites, CTAs induce humoral as well as cell-mediated immune responses when aberrantly expressed in somatic cells; as such, CTAs have emerged as highly attractive targets for cancer immunotherapy (2). Vaccines targeting CTAs such as NY-ESO-1, MAGE-A1, and MAGE-A3 induce antitumor immunity, and T cells expressing native or genetically engineered receptors recognizing these antigens mediate tumor regression in some cancer patients (3–5).

Approximately 50% of CT genes, including *NY-ESO-1*, *MAGE-A1*, and *MAGE-A3*, are located on the X chromosome (6). CT-X chromosome (CT-X) genes are normally expressed in spermatogonia, and typically comprise extended families associated with inverted DNA repeats (7). Relative to autosomal CT genes, CT-X genes are more frequently activated in cancer cells, and particular gene families appear to be derepressed in a tumor-specific manner. Although believed to be activated as a result of global DNA demethylation, the epigenetic mechanisms mediating coordinate derepression of CT genes during multistep carcinogenesis have not been fully elucidated (7–9).

Although NY-ESO-1, MAGE-A1, and MAGE-A3 are expressed in 25% to 40% of non–small cell lung cancers (NSCLC; ref. 10), immune responses to these CTAs are uncommon in lung cancer patients (11, 12) due, in part,

Authors' Affiliations: Sections of [1]Thoracic Oncology and [2]Tumor Immunology, Surgery Branch, Center for Cancer Research; and [3]Chemical Biology Laboratory, National Cancer Institute, Bethesda, Maryland

Note: Supplementary data for this article are available at Cancer Research Online (http://cancerres.aacrjournals.org/).

Corresponding Author: David S. Schrump, Head, Thoracic Oncology Section, Surgery Branch, Center for Cancer Research, National Cancer Institute, 10 Center Drive, Rm 4-3942 MSC 1201, Bethesda, MD 20892. Phone: 301-496-2128; Fax: 301-451-6934; E-mail: david_schrump@nih.gov

doi: 10.1158/0008-5472.CAN-10-2442

to levels of antigen expression, which are below the threshold for immune recognition. Conceivably, upregulation of CTA expression by chromatin-remodeling agents can enhance immunogenicity of lung cancer cells, facilitating their eradication by endogenous immune mechanisms, or adoptively transferred T cells. Previously, we showed that the DNA-demethylating agent, 5-aza-2′-deoxycytidine (decitabine; DAC) and the histone deacetylase (HDAC) inhibitor depsipeptide (romidepsin; DP) mediate synergistic activation of CT-X gene expression in cultured lung cancer cells but not in normal epithelia or lymphoid cells (8). In addition, we reported that, following DAC or sequential DAC/DP exposure, lung cancer cells can be recognized by cytolytic T lymphocytes (CTL) expressing receptors specific for NY-ESO-1 or MAGE-A3 (13–15). Furthermore, we have shown upregulation of *NY-ESO-1* and *MAGE-A3* expression in primary lung cancers in patients receiving 72-hour continuous decitabine infusions (steady-state plasma concentrations ~50–100 nmol/L; ref. 16; Schrump and colleagues, manuscript in preparation). Finally, we have shown that a CTA induced in tumor cells *in vivo* by systemic DAC administration can be effectively targeted by adoptively transferred CTL in immunocompetent mice (17). The present study was undertaken to comprehensively examine mechanisms regulating *NY-ESO-1*, *MAGE-A1*, and *MAGE-A3* expression in lung cancer cells to further develop epigenetic strategies for human cancer immunotherapy.

Materials and Methods

Cell lines and drug treatment conditions

All lung cancer lines were obtained from the American Type Culture Collection and were characterized and authenticated at the repository by methods including mycoplasma testing, DNA profiling, and cytogenetic analysis; these lines were used within 6 months of purchase for this study, validated in our laboratory by periodic human leukocyte antigen (HLA) typing, and cultured as described (8). Primary normal human bronchial epithelial (NHBE) cells, small airway epithelial cells (SAEC), and normal human dermal fibroblasts (NHDF) were purchased from Lonza, Inc., and cultured according to manufacturer's instructions. Immortalized human bronchial epithelial cells (HBEC) were generously provided by John D. Minna (University of Texas Southwestern, Dallas, TX) and cultured as described (18). DAC and trichostatin A (TSA) were purchased from Sigma Chemical Company. DZNep was provided by the Chemical Biology Laboratory, National Cancer Institute (NCI). DP was obtained from the Developmental Therapeutics Program, NCI. The effects of DAC and DZNep treatment on CT-X gene expression were determined after exposure to 0.1 μmol/L DAC or 0.5 to 5 μmol/L DZNep for 72 hours or concurrent DAC–DZNep (0.1:0.5 μmol/L) for 72 hours followed by exposure to normal media for 18 to 24 hours. DAC/DP and DAC/TSA treatments were carried out as described (8).

Real-time reverse transcription-PCR analysis

RNA was isolated using RNeasy Mini Kit (Qiagen). cDNAs were made using Reverse Transcription Kit (Bio-Rad). Quantitative reverse transcription (qRT)-PCR primers for CT-X genes and β-actin expression are listed in Supplementary Table S1.

Immunoblot analysis

Total cell proteins were extracted and immunoblotting was carried out as described previously (19) with minor modifications, using primary antibodies listed in Supplementary Table S2 including appropriate horseradish peroxidase–conjugated secondary antibodies, and SuperSignal West Pico Chemiluminescent Substrate (Pierce Biotechnology). Testis lysate (Abcam) was used as positive control for NY-ESO-1 and MAGE-A1. Lysates from HEK293 cells constitutively expressing MAGE-A3 were used as a positive control for this CTA (15).

Immunofluorescence analysis

NY-ESO-1, *MAGE-A1*, and *MAGE-A3* expression in cultured cells was detected by immunofluorescence techniques using primary antibodies recognizing these CTAs (Supplementary Table S2) and visualized using fluorescein isothiocyanate (FITC)-labeled secondary antibodies (Supplementary Table S2) as described (20). Nuclei were counterstained with 4′,6-diamidino-2-phenylindole (DAPI).

Pyrosequencing analysis

CpG islands within the *NY-ESO-1*, *MAGE-A1*, and *MAGE-A3* promoters were identified using an online CpG island search engine (21). Genomic DNA was isolated from drug-treated or control cells using the Qiagen DNeasy Kit. Bisulfite modification of DNA was done using the Qiagen EpiTect Bisulfite Kit. Pyrosequencing was done as described previously (18), using primers listed in Supplementary Table S1.

Chromatin immunoprecipitation assay

Chromatin immunoprecipitation (ChIP) assay was conducted as described (22) with minor modifications. Briefly, DNA–protein complexes were cross-linked with formaldehyde at a final concentration of 1% for 15 minutes. Immune complexes were formed with either nonspecific immunoglobulin G (IgG) or ChIP-grade antibodies listed in Supplementary Table S2. DNA was eluted and purified from complexes, followed by PCR amplification of the *NY-ESO-1*, *MAGE-A1*, or *MAGE-A3* promoters as previously described (8), using primers listed in Supplementary Table S1.

Generation of *KMT6*, *KDM1*, *KDM5B*, or *SirT1* knockdown cells and KMT6-overexpressing stable cells

H841 cells were transduced with lentiviral short hairpin RNA (shRNA) vectors targeting *KMT6*, *KDM1*, *KDM5B*, and *SirT1* or sham sequences (Sigma), or transfected with pCMV6-AC-GFP or pCMV6-AC-GFP-KMT6 (Origene). Target gene knockdown or overexpression was confirmed by RT-PCR and immunoblot. Stable transfectants (4 independent clones for each knockdown or overexpression) were isolated and expanded under puromycin (knockdowns) or G418 selection (overexpressors). Following reconfirmation of target gene knockdown or overexpression, individual clones were pooled for subsequent experiments.

Retroviral transduction of tumor cell lines with HLA-A*0201 and peripheral blood lymphocytes with T-cell receptor (TCR) genes against NY-ESO-1 or MAGE-A3 was carried out. H1299 or H841 lung cancer cells, SAECs, HBECs, or NHDFs were transduced with a retroviral vector expressing cDNA of HLA-A*0201 (23). H1299 and H841 cell lines stably expressing HLA-A*0201 were expanded under G418 selection. Peripheral blood lymphocytes (PBL) expressing HLA-A*0201–restricted TCRs recognizing NY-ESO-1 or MAGE-A3 were generated as described (14, 15).

Cytokine release assays

Drug-treated or control tumor cells with or without *HLA-A*0201* expression were cocultured with untransduced or MAGE-A3 or NY-ESO-1 TCR-transduced lymphocytes; IFN-γ secretion in supernatants was measured by ELISA as described (14, 15).

Chromium release assays

The ability of NY-ESO-1– or MAGE-A3–specific TCR-transduced PBL to lyse HLA-A*0201$^+$ lung cancer or normal lung cell targets was measured using chromium (^{51}Cr) release assays. Briefly, after DAC, DZNep, or DAC–DZNep exposure, H2087 and H841-A*0201 or H1299-A*0201 and their respective controls were cocultured with effector cells, with subsequent analysis of ^{51}Cr release as described (15, 23).

Results

Expression profiles of CT-X genes in lung cancer cells

Preliminary qRT-PCR experiments were conducted to examine CT-X gene expression in cultured lung cancer cells as well as normal or immortalized respiratory epithelial cells (Supplementary Table S3). This analysis, which revealed heterogeneous CT-X gene expression in NSCLC and small cell lung cancer (SCLC) cells, but not normal respiratory epithelia, allowed us to choose several cell lines for further study (Fig. 1A; left). Relative to control testis cells, H1299 cells exhibit high-level expression of *NY-ESO-1*, *MAGE-A1*, and *MAGE-A3*. In contrast, H841 cells do not express *NY-ESO-1*, *MAGE-A1*, or *MAGE-A3*. A549 and Calu-6 cells exhibit moderate levels of *MAGE-A3*, but do not express *NY-ESO-1* or *MAGE-A1*. NHBE cells and SAEC do not express any CT-X genes. Immunoblot analysis (Fig. 1A; right) confirmed results of these qRT-PCR experiments.

Chromatin structure relative to CT-X gene expression in lung cancer cells

Pyrosequencing and ChIP experiments were undertaken to examine DNA methylation and a variety of histone marks in lung cancer cells exhibiting differential CT-X gene expression. Pyrosequencing experiments (Fig. 1B) revealed that the *NY-ESO-1* and *MAGE-A1* promoters were hypermethylated in A549, Calu-6, and H841 lung cancer cells and NHBE cells; these promoters were hypomethylated in H1299 cells. In contrast, the *MAGE-A3* promoter was hypermethylated in H841 and NHBE cells, partially methylated in A549 and Calu-6 cells, and demethylated in H1299 cells. These findings were consistent with results of previously described qRT-PCR and immunoblot experiments. Although demethylation of *MAGE-A3* appeared to coincide with demethylation of D4Z4, no consistent relationship was evident with regard to *NY-ESO-1*, *MAGE-A1*, or *MAGE-A3* promoter demethylation and global DNA demethylation assessed by pyrosequencing of NBL2, D4Z4, and LINE-1 repetitive DNA sequences, possibly attributable to incomplete analysis of these regions by pyrosequencing methods.

ChIP experiments were conducted to further investigate epigenetic phenomena associated with repression/activation of *NY-ESO-1*, *MAGE-A1*, and *MAGE-A3* in lung cancer cells. As shown in Fig. 1C, the *NY-ESO-1*, *MAGE-A1*, and *MAGE-A3* promoters in H1299 cells exhibited increased occupancy of RNA polymerase II (Pol II), enrichment of euchromatin/activation marks, such as H3K4Me2, H3K4Me3, H3K79Me2, total H3Ac, H3K9Ac, total H4Ac, and H4K16Ac, and decreased occupancy of SirT1 as well as polycomb repressor complex (PRC)-2 components (KMT6, EED, and SUZ-12), and the associated PRC-2–mediated repression mark, H3K27Me3. In contrast, RNA Pol II and histone-activation marks were markedly diminished, whereas SirT1, PRC-2 components, and H3K27Me3 levels were considerably higher within the *NY-ESO-1* and *MAGE-A1* promoters in A549, Calu-6, H841, and NHBE cells, all of which do not express these CT-X genes. Variable levels of RNA Pol II and activation/repression marks were present within the *MAGE-A3* promoter in A549, Calu-6, H841, and NHBE cells, consistent with levels of expression of this CT-X gene in these cells. No consistent relationship was observed between activation/repression of these CT-X genes and H3K9Me3, previously considered to be a mark of stable, silenced heterochromatin (24), but more recently shown to coincide with RNA Pol II–mediated gene activation (25). Densitometry results of these ChIP experiments are summarized in Supplementary Table S4. Collectively, these experiments established that differential repression of *NY-ESO-1*, *MAGE-A1*, and *MAGE-A3* in lung cancer cells is attributable to persistence of apparently normal heterochromatin structure within the promoters of these CT-X genes. Furthermore, levels of euchromatin marks, particularly H3K79Me2, appear to coincide with magnitude of CT-X gene derepression in lung cancer cells.

Effects of histone lysine methylation on CT-X gene expression

Our previous studies have shown that pharmacologic inhibition of histone lysine deacetylation enhances CT-X gene activation by DNA-demethylating agents (10). Therefore, additional experiments were conducted to ascertain whether modulation of histone lysine methylation alters CT-X gene expression in lung cancer cells. Briefly, lentiviral shRNA-transduction techniques were used to knock down *LSD-1* (*KDM1*) and *JARID1B* (*KDM5B*) that mediate demethylation of mono-, di-, and trimethylated H3K4 (26, 27), or the histone lysine methyltransferase *KMT6* that mediates trimethylation of H3K27 (28) in H841 cells; these cells were chosen for analysis because they do not express *NY-ESO-1*, *MAGE-A1*, or *MAGE-A3*. Preliminary qRT-PCR and immunoblot experiments showed approximately 50% to 70% reduction in target gene expression by the respective shRNAs relative to controls (Fig. 2A; left). Immunoblot analysis (Fig. 2A; right) showed

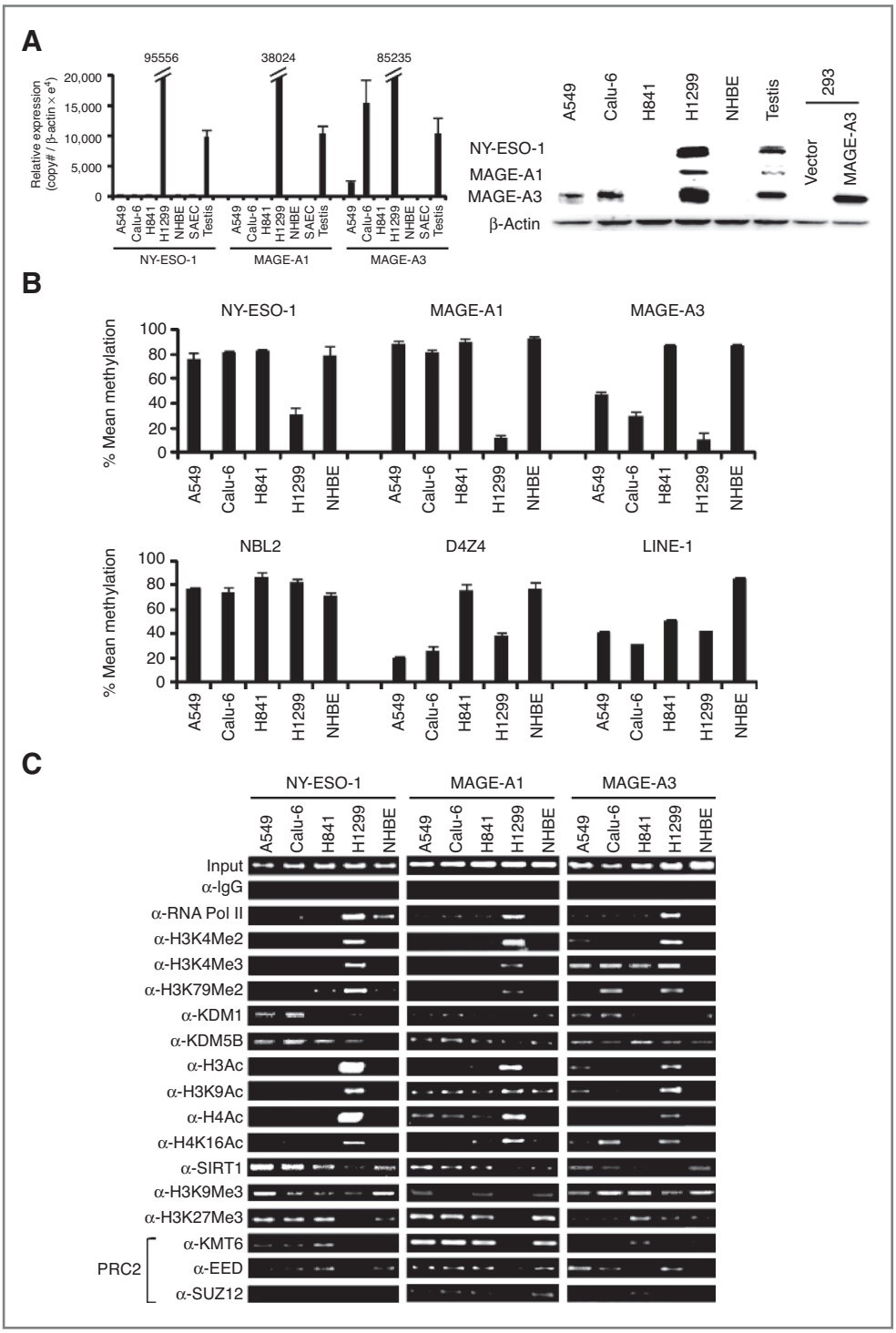

Figure 1. A, left, qRT-PCR analysis of *NY-ESO-1*, *MAGE-A1*, and *MAGE-A3* expression in cultured lung cancer cells, NHBE cells, SAECs, and control testis cells. Results are expressed as mean ± SD of 3 independent experiments. Right, immunoblot analysis depicting expression of NY-ESO-1, MAGE-A1, and MAGE-A3 in A549, Calu-6, H841, and H1299 lung cancer cells and NHBE cells. Testis protein lysate was used as positive control for NY-ESO-1 and MAGE-A1. For MAGE-A3, protein lysate from HEK293 overexpressing MAGE-A3 was used as a positive control because the MAGE-A3 antibody exhibits low-level cross-reactivity with other related MAGE A proteins. B, methylation status of *NY-ESO-1*, *MAGE-A1*, *MAGE-A3*, *NBL2*, *D4Z4*, and *LINE-1* sequences in A549, Calu-6, H841, and H1299 lung cancer and NHBE cells as measured by pyrosequencing. Results are expressed as mean ± SD of 3 independent experiments. C, ChIP analysis of the *NY-ESO-1*, *MAGE-A1*, and *MAGE-A3* promoters in A549, Calu-6, H841, and H1299 lung cancer and NHBE cells. Presence of activation (euchromatin) marks and decreased repressive marks within the *NY-ESO-1*, *MAGE-A1*, and *MAGE-A3* promoters coincided with activation of these CT-X genes. See text for further details.

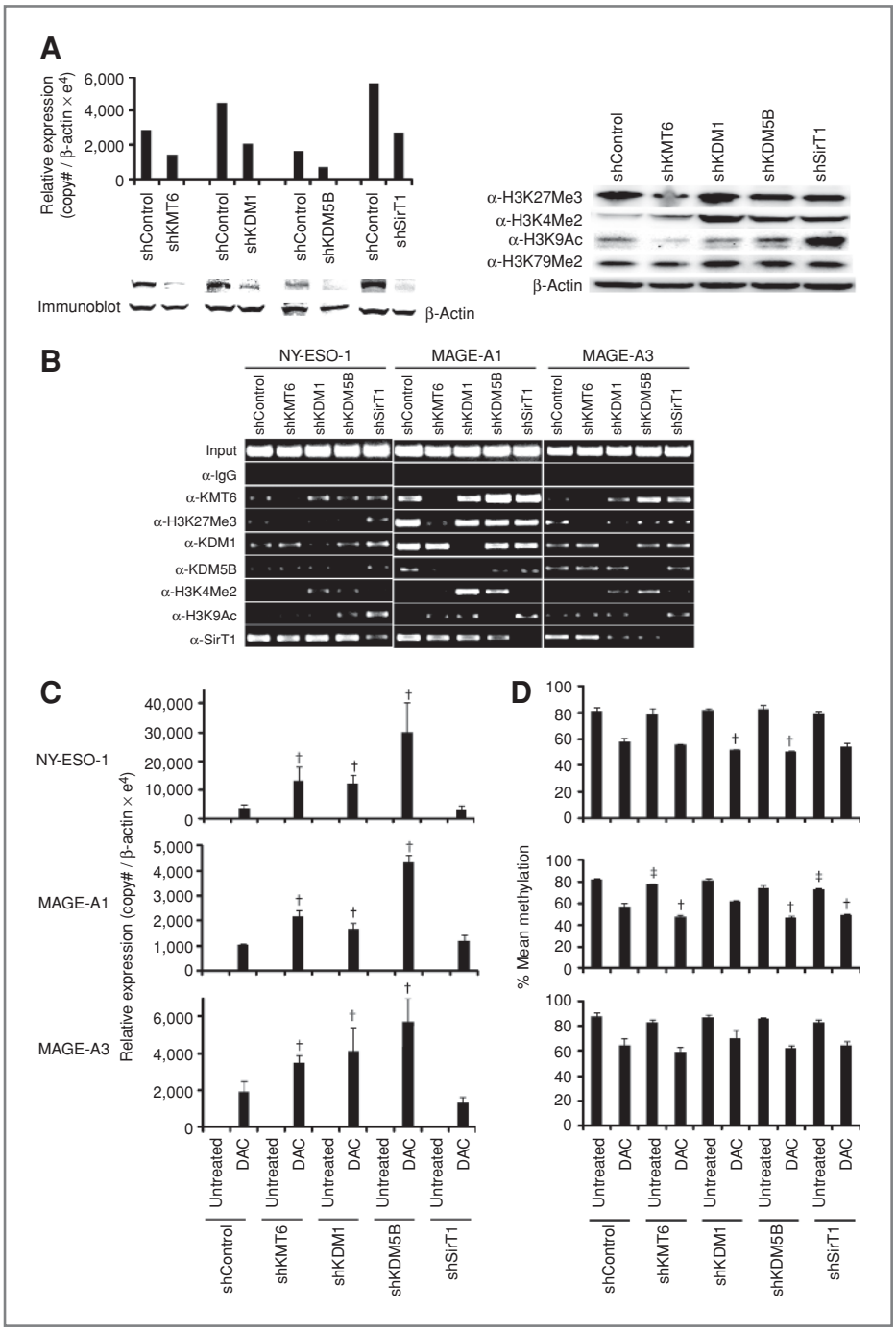

Figure 2. A, left, qRT-PCR (top) and immunoblot analysis (bottom) of KMT6, KDM1, KDM5B, and SirT1 in H841 cells transfected with shRNAs against respective targets or sham control sequences, showing target gene knockdown. Right, immunoblot analysis showing that knockdown of KMT6 and SirT1 leads to decreased levels of H3K27Me3 and H3K9Ac, respectively, whereas knockdown of KDM1 and KDM5B results in increased global H3K4Me2 levels. As expected, no changes in global H3K79Me2 levels were seen in these knockdowns. B, ChIP analysis of the *NY-ESO-1*, *MAGE-A1*, and *MAGE-A3* promoters in knockdown of *KMT6*, *KDM1*, *KDM5B*, and *SirT1* in H841 cells. Knockdown of *KMT6* and *SirT1* was associated with decreased occupancy of these histone modifiers, with corresponding changes in H3K27Me3 and H3K9Ac, respectively; knockdown of *KDM1* and *KDM5B* decreased occupancy of these histone methyltransferases with a corresponding increase in H3K4Me2 within the *NY-ESO-1*, *MAGE-A1*, and *MAGE-A3* promoters. C, qRT-PCR analysis showing that *KMT6*, *KDM1*, and *KDM5B* knockdown significantly enhances DAC-mediated activation of *NY-ESO-1*, *MAGE-A1*, and *MAGE-A3* in H841 cells. Effects of *SirT1* knockdown were considerably less pronounced in these cells. The bars represent mean ± SD of triplicate experiments. †, $P < 0.05$ versus DAC-shControl. D, pyrosequencing analysis of *NY-ESO-1*, *MAGE-A1*, and *MAGE-A3* promoter methylation in H841 cells with or without knockdown of *KMT6*, *KDM1*, *KDM5B*, or *SirT1* exposed to normal media or DAC. Knockdown of these histone modifiers had variable and relatively modest effects on methylation status of these CT-X promoters. †, $P < 0.05$ versus DAC-shControl; ‡, $P < 0.05$ versus untreated shControl.

decreased global H3K27Me3 and increased global H3K9Ac in *KMT6* and *SirT1* knockdowns, respectively, relative to control cells. Increased global levels of H3K4Me2 were evident in *KDM1* and *KDM5B* knockdowns relative to control cells; interestingly, an increase in this activation mark was also observed in *SirT1* knockdown cells. ChIP experiments revealed that global changes in these activation and repression marks tended to coincide with similar alterations and decreased occupancy of the respective histone modifiers in the *NY-ESO-1*, *MAGE-A1*, and *MAGE-A3* promoters in knockdowns relative to control cells (Fig. 2B). Subsequent qRT-PCR experiments revealed that knockdown of *KMT6*, *KDM1*, or *KDM5B* alone was insufficient to activate *NY-ESO-1*, *MAGE-A1*, or *MAGE-A3* in H841 lung cancer cells. However, knockdown of *KMT6*, *KDM1*, or *KDM5B* enhanced DAC-mediated induction of these CT-X genes approximately 3- to 11-fold in these cells (Fig. 2C); knockdown of *KDM5B* appeared to have the most effect with regard to potentiation of DAC-mediated CT-X gene activation in lung cancer cells. The effects of targeted modulation of histone lysine methylation appeared more pronounced than those observed following knockdown of the class III HDAC, *SirT1*.

Additional pyrosequencing experiments were conducted to ascertain whether modulation of histone lysine methylation affected DNA-methylation status of *NY-ESO-1*, *MAGE-A1*, and *MAGE-A3* in DAC-treated and control lung cancer cells. Results of this analysis are depicted in Fig. 2D. Effects of histone methylation changes varied somewhat among the 3 CT-X genes. In general, the effects of *KMT6*, *KDM1*, or *KDM5B* knockdown on *NY-ESO-1*, *MAGE-A1*, or *MAGE-A3* promoter methylation were modest, and did not directly coincide with magnitude of enhancement of DAC-mediated activation of these CT-X genes. A similar phenomenon was observed following knockdown of *SirT1* in H841 cells.

Effects of DZNep on CT-X gene expression

Additional experiments were conducted to ascertain whether pharmacologic agents in preclinical development could recapitulate the previously described effects of histone lysine methylation on DAC-mediated activation of CT-X genes. Our studies focused on DZNep, a novel inhibitor of PRC-2 expression (29). Briefly, lung cancer cells were cultured for 72 hours in normal media with or without DAC (0.1 μmol/L), DZNep (0.5 or 5 μmol/L), or concurrent DAC–DZNep (0.1:0.5 μmol/L) followed by analysis after 24 hours. Preliminary immunoblot experiments showed that DZNep mediated dose-dependent depletion of KMT6, EED, and SUZ-12 with concomitant reduction in global H3K27Me3 levels in H841 cells (Fig. 3A; left); qRT-PCR experiments revealed that DZNep mediated modest dose-dependent reductions in *KMT6* and *SUZ12* but not *EED* mRNA levels (Fig. 3A; right). Additional experiments showed that low-dose DZNep (0.5 μmol/L—approximately 1 log lower than the cytotoxic dose of this agent in cancer cells) mediated very modest activation of *NY-ESO-1*, *MAGE-A1*, and *MAGE-A3* in H841 cells; in contrast, DZNep significantly enhanced DAC-mediated CT-X gene activation in these cells (Fig. 3B). Immunofluorescence experiments confirmed that DZNep enhanced DAC-mediated expression of NY-ESO-1, MAGE-A1, and MAGE-A3 in H841 cells (Fig. 3C). This phenomenon extended to other CT-X genes such as *MAGE-A12* (Fig. 3B), and was observed in other lung cancer lines (Supplementary Table S5). The magnitude of enhancement of DAC-mediated derepression of CT-X genes in cancer cells by DZNep was markedly higher than that observed in SAECs (Fig. 3B) or NHBE cells (data not shown). Relative to normal SAECs, immortalized HBECs appeared more responsive to DAC and DZNep; however, DZNep did not appear to augment DAC-mediated CT-X gene activation in these cells. The magnitude of DAC–DZNep–mediated CT-X gene induction in lung cancer cells approximated or exceeded that observed following sequential DAC–DP or DAC–TSA treatment; addition of TSA or DP did not consistently improve CT-X gene activation mediated by low-dose DAC–DZNep (Supplementary Table S5).

Effects of DZNep on DNA methylation and H3K27Me3 within CT-X gene promoters

Pyrosequencing and ChIP analyses were conducted to further examine the mechanisms by which DZNep modulates CT-X gene expression in lung cancer cells. Results of these experiments are depicted in Fig. 4. NHBE and H1299 cells were used as positive and negative methylation controls, respectively. As anticipated, DAC-mediated activation of *NY-ESO-1*, *MAGE-A1*, and *MAGE-A3* coincided with significant demethylation of the respective promoters. In contrast to what was observed following histone lysine methyltransferase knockdown (Fig. 2D), DZNep alone mediated a modest, but significant, demethylation of all 3 CT-X gene promoters (Fig. 4A); in combination with DAC, DZNep exhibited an additive demethylation effect in the *NY-ESO-1* and *MAGE-A3* promoters (Fig. 4A). The effects of DAC, DZNep, or DAC–DZNep on *NY-ESO-1*, *MAGE-A1*, and *MAGE-A3* promoters coincided with similar effects on global DNA methylation assessed by pyrosequencing analysis of NBL2, D4Z4, and LINE-1 sequences (Fig. 4B). Subsequent ChIP experiments confirmed that DZNep decreased KMT6 and H3K27Me3 levels within the *NY-ESO-1*, *MAGE-A1*, and *MAGE-A3* promoters (Fig. 4C); the magnitude of decrease in KMT6 and H3K27Me3 levels appeared to coincide with extent of demethylation and derepression of these promoters.

Effects of KMT6 overexpression on CT-X gene activation mediated by DZNep

Additional experiments were undertaken to specifically examine whether the effects of DZNep on DAC-mediated activation of CT-X genes were attributable, at least in part, to depletion of KMT6. Briefly, H841 cells stably expressing *KMT6* were treated with DAC, DZNep, or DAC–DZNep as previously described. Immunoblot analysis (Fig. 5A; left) showed increased global levels of KMT6 and H3K27Me3 in KMT6-transfected H841 cells relative to vector controls. DZNep markedly depleted KMT6 and H3K27Me3 levels in KMT6 overexpressors, and qRT-PCR experiments showed a modest, but statistically insignificant, diminution of *KMT6* expression by DZNep (Fig. 5A; right). Additional qRT-PCR experiments revealed that overexpression of *KMT6*

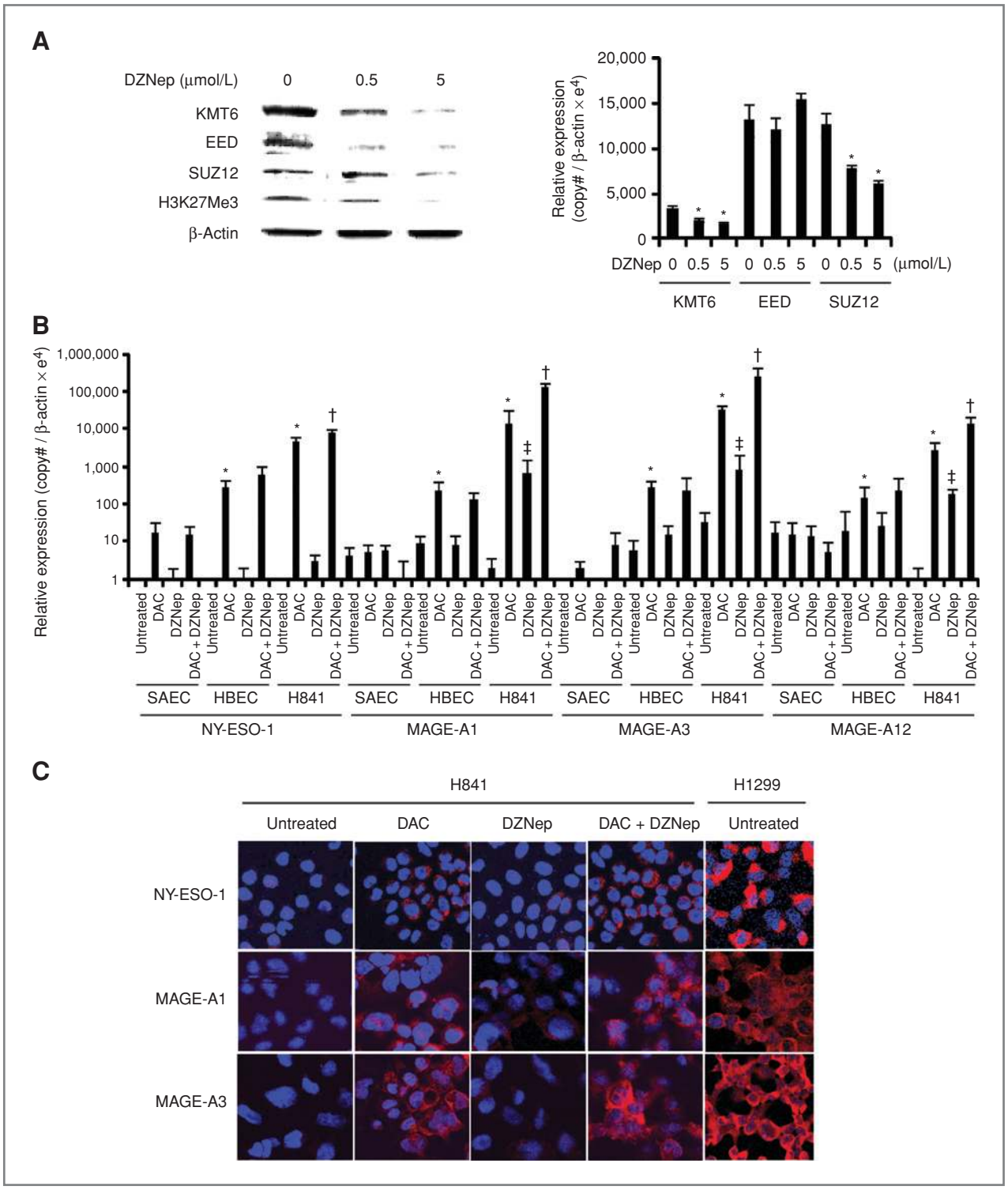

Figure 3. A, left, immunoblot analysis showing dose-dependent depletion of KMT6, EED, and SUZ12 and reduced global H3K27Me3 levels in H841 cells mediated by DZNep. Right, qRT-PCR analysis of *KMT6*, *EED*, and *SUZ12* levels in H841 cells following 72-hour DZNep exposure. *, $P < 0.05$, DZNep-treated versus untreated cells. B, qRT-PCR analysis of *NY-ESO-1*, *MAGE-A1*, and *MAGE-A3* expression in cultured cells following DAC, DZNep, or DAC–DZNep treatment. Modest CT-X gene activation was seen in immortalized HBEC cells but not in SAECs. The bars represent the mean ± SD of triplicate experiments. *, $P < 0.05$, DAC-treated versus untreated cells; †, $P < 0.05$, DAC–DZNep treated versus DAC-treated cells; ‡, $P < 0.05$, DZNep-treated versus untreated cells. C, immunofluorescence analysis of NY-ESO-1, MAGE-A1, and MAGE-A3 expression in H841 cells following DAC, DZNep, or DAC–DZNep exposure. H1299 was used as a positive control.

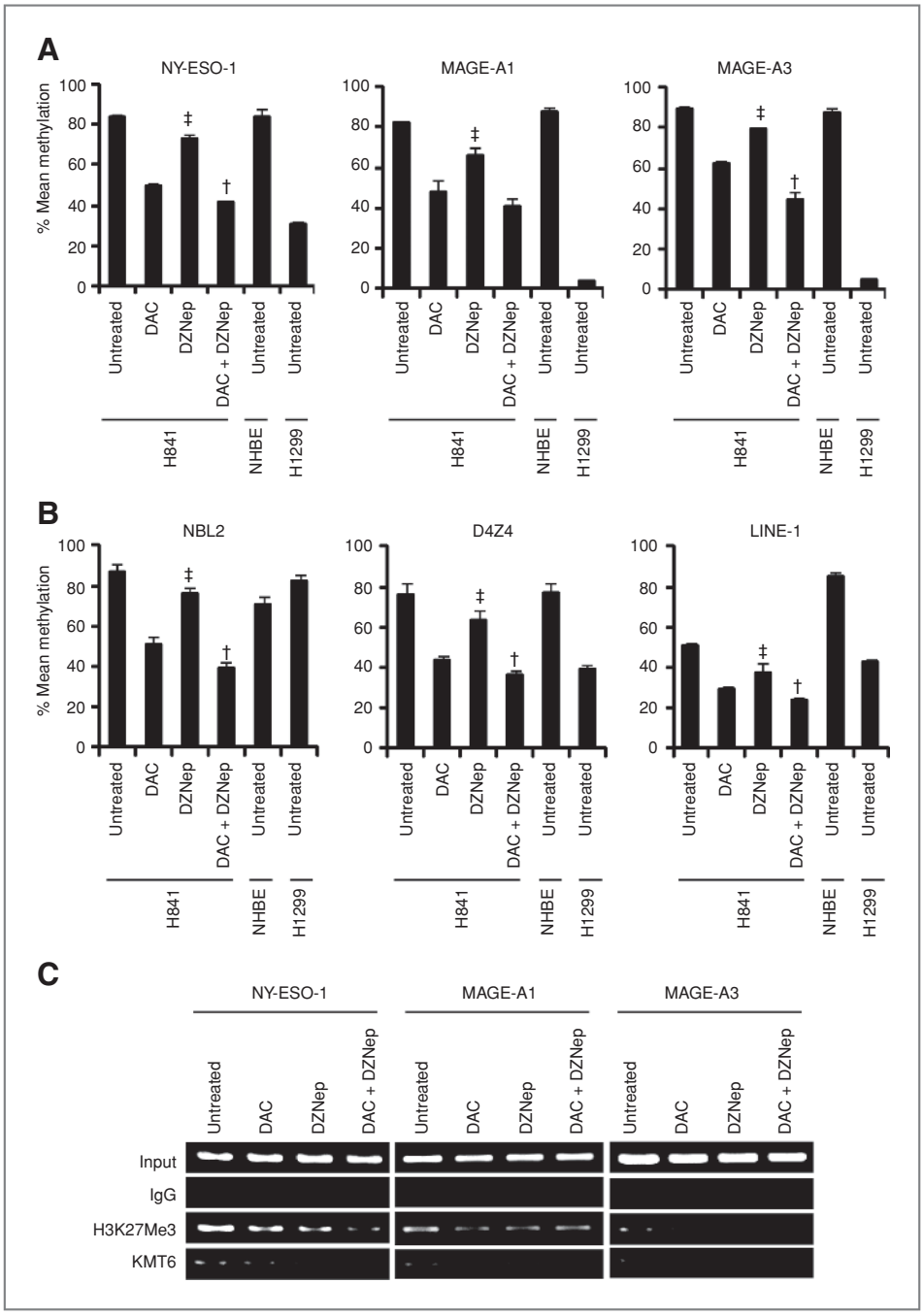

Figure 4. A and B, pyrosequencing analysis of *NY-ESO-1*, *MAGE-A1*, and *MAGE-A3* promoters and *NBL2*, *D4Z4*, and *LINE-1* methylation in H841 cells following treatment with DAC, DZNep, or DAC–DZNep. Relative to treatment with either agent alone, DAC–DZNep appeared to exert a modest additive effect on demethylation of these sequences. CT-X promoter demethylation appeared to coincide with global DNA demethylation mediated by the treatment regimens. †, $P < 0.05$, DAC + DZNep versus DAC; ‡, $P < 0.05$, DZNep-treated versus untreated cells. C, ChIP analysis showing reduced KMT6 and H3K27Me3 levels within the *NY-ESO-1*, *MAGE-A1*, and *MAGE-A3* promoters in H841 cells following treatment with DAC, DZNep, or DAC–DZNep. Concurrent DAC–DZNep treatment appeared to markedly decrease KMT6 and H3K27Me3 levels within these promoters.

significantly attenuated the enhancement effect of DZNep on DAC-mediated induction of *NY-ESO-1*, *MAGE-A1*, or *MAGE-A3* (Fig. 5B).

Recognition of lung cancer cells by NY-ESO-1– and MAGE-A3–specific TCR-engineered T cells following DZNep exposure

Additional experiments were conducted to examine whether DZNep enhances immunogenicity of lung cancer cells. Briefly, H2087 lung cancer cells, which endogenously express *HLA-A*0201*, and SAECs (chosen because they proliferate faster than NHBE cells) and H841 cells transduced with *HLA-A*0201* (SAEC-A2 and H841-A2, respectively) were exposed to NM, DAC, DZNep, or DAC–DZNep as previously described, and subsequently cocultured with TCR-engineered PBL recognizing *NY-ESO-1* or *MAGE-A3* in the context of HLA-A*0201. Representative results from 2 independent experiments conducted using PBL from 2 different patients are depicted in Fig. 6. For these experiments, H1299 and H1299-A2 cells served as negative and positive controls,

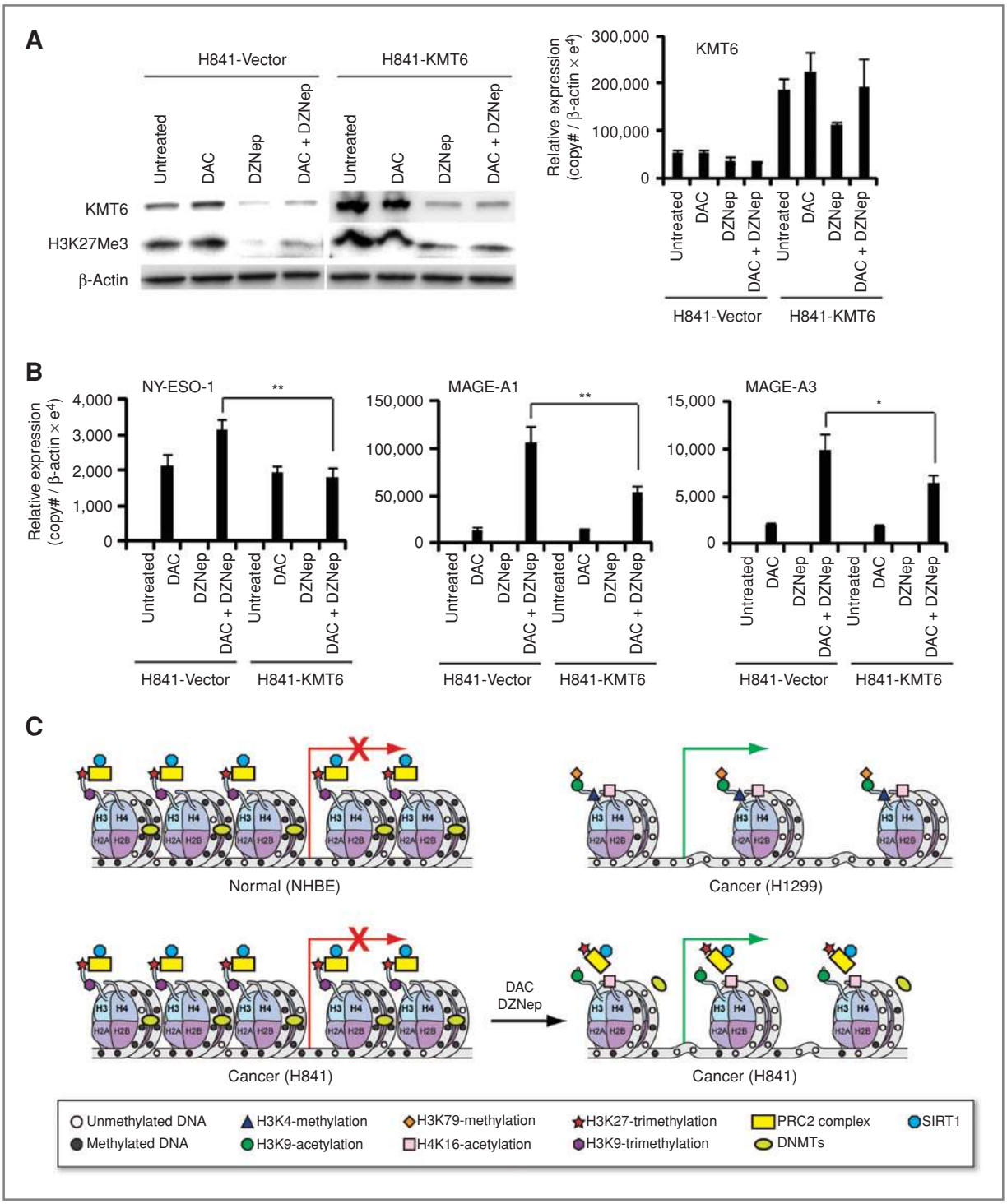

Figure 5. A, Left, immunoblot analysis showing DZNep significantly reduces KMT6 and H3K27Me3 protein levels in H841 cells overexpressing KMT6 (H841-KMT6) as well as vector controls. Right, qRT-PCR analysis of KMT6 in H841-KMT6 cells. B, qRT-PCR analysis revealing significant attenuation of DAC–DZNep-mediated activation of *NY-ESO-1*, *MAGE-A1*, and *MAGE-A3* expression in H841-KMT6 cells relative to vector controls following treatment with DAC–DZNep. The bars represent mean ± SD of triplicate experiments. *, $P < 0.05$; **, $P < 0.005$. C, epigenetic modification patterns of CT-X genes in normal and cancer cells. In NHBE and H841 lung cancer cells, which do not express *NY-ESO-1*, *MAGE-A1*, or *MAGE-A3*, respective promoters exhibit hypermethylated DNA, occupancy of PRC-2–SirT1 complex, and repressive heterochromatin marks such as H3K9Me3 and H3K27Me3. H1299 lung cancer cells expressing these CT-X genes exhibit hypomethylated DNA, dissociation of PRC-2-SIRT1, decreased heterochromatin marks, and presence of euchromatin marks such as H3K4Me2/3 and H3K9Ac within the respective promoters. DAC/DZNep treatment activates CT-X gene promoters by inhibiting DNA methyltransferase and PRC-2 activity.

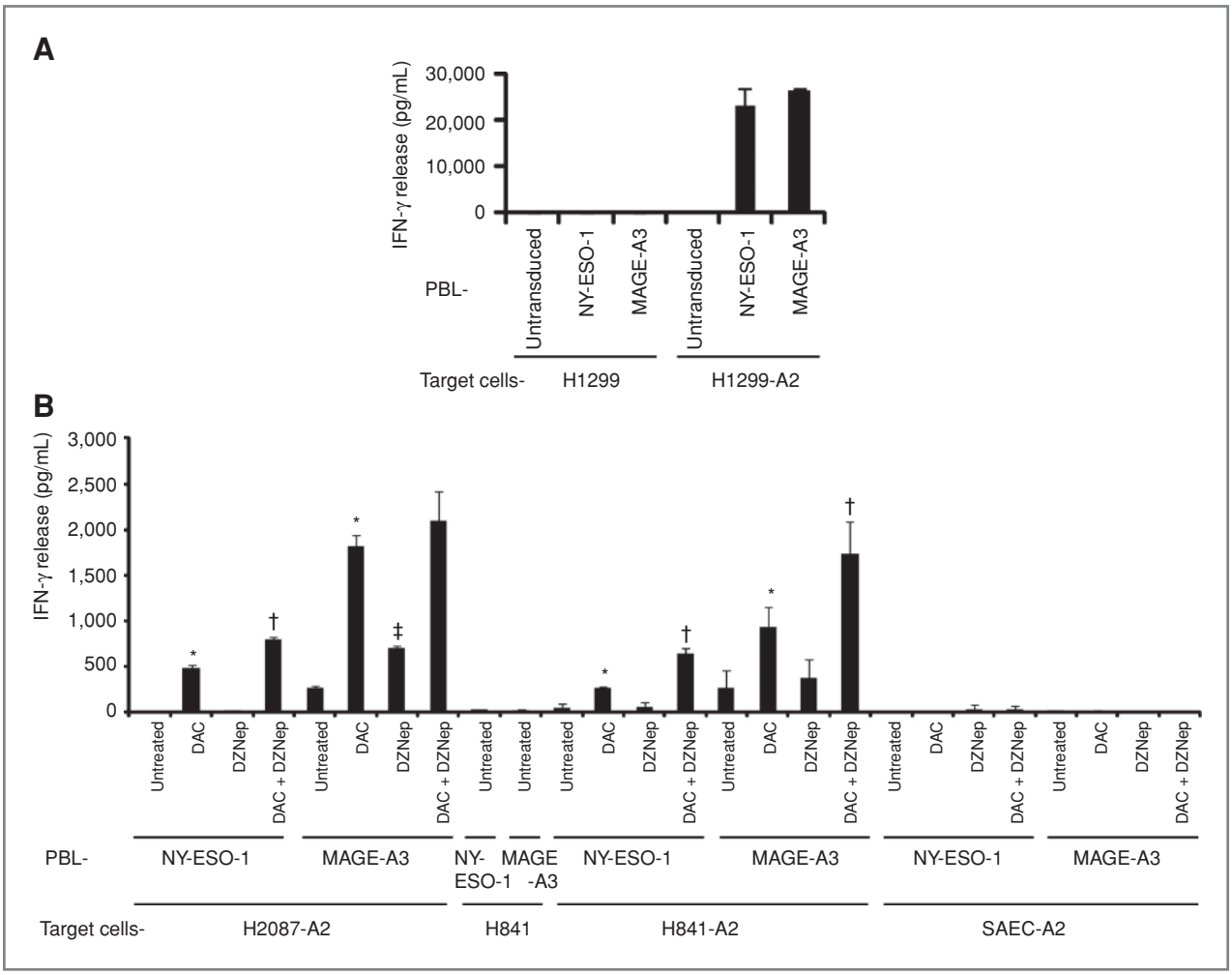

Figure 6. A, IFN-γ release by HLA-restricted CTLs recognizing *NY-ESO-1* and *MAGE-A3* in the context of HLA-A*A0201 after overnight incubation with H1299 or H1299-A2 targets (negative and positive controls, respectively). B, IFN-γ release by HLA-restricted CTLs specific for NY-ESO-1 and MAGE-A3 after overnight incubation with H2087, as well as with H841-A2 and SAEC-A2. Targets represent untreated controls, or cells exposed to DAC (0.1 μmol/L), DZNep (0.5 μmol/L), or DAC–DZNep (0.1:0.5 μmol/L). Data are representative of 2 independent experiments conducted with 2 different PBL donors. *, $P < 0.05$, DAC-treated versus untreated cells; †, $P < 0.05$, DAC–DZNep versus DAC; ‡, $P < 0.05$ DZNep-treated versus untreated cells.

respectively (Fig. 6A). As shown in Fig. 6B, increased IFN-γ release was observed following coculture of NY-ESO-1 and MAGE-A3 effector cells with H2087 and H841-A2 cells previously exposed to DAC, which was significantly augmented by concomitant exposure to DZNep (0.5 μmol/L). Very low-level cytokine release was observed following coculture of effector cells with DZNep-treated H2087 and H841-A2 targets. The magnitude of enhancement of DAC-mediated cytokine release by DZNep was more pronounced for MAGE-A3 relative to NY-ESO-1 effector cells; these results were consistent with qRT-PCR analysis of CT-X gene expression in target cells following drug treatment. Background levels of IFN-γ release were observed following coculture of effector cells with parental untreated H1299 cells, or drug-treated H841 cells lacking *HLA-A*0201* expression. Effector cells did not recognize either drug-treated *HLA-A*0201*–transduced SAECs (Fig. 6B) or HBECs and NHDF (data not shown), presumably due to very low levels of NY-ESO-1 and MAGE-A3 induction in these cells by the treatment regimen (Supplementary Table S6).

Chromium release experiments were conducted to evaluate lysis of H841-A2 cells by MAGE-A3– or NY-ESO-1–specific effector cells. Representative results from 2 independent experiments conducted using PBL from 2 different donors are depicted in Fig. 7. H1299-A2 and parental H1299 cells served as positive and negative controls, respectively (Fig. 7A). Low-level lysis was observed following coculture of untransduced effector cells with H841 targets possibly due to nonspecific alloreactivity, recognition of tumor targets by endogenous T-cell receptors, presence of natural killer cells, and mild toxicity of the drug-treatment regimens (Fig. 7B). Compared with untreated controls, DAC-treated H841-A2 cells were more efficiently lysed by the effector cells (Fig. 7C). Interestingly, DZNep treatment also led to increased lysis of H841-A2 cells, whereas the percentage of specific lysis

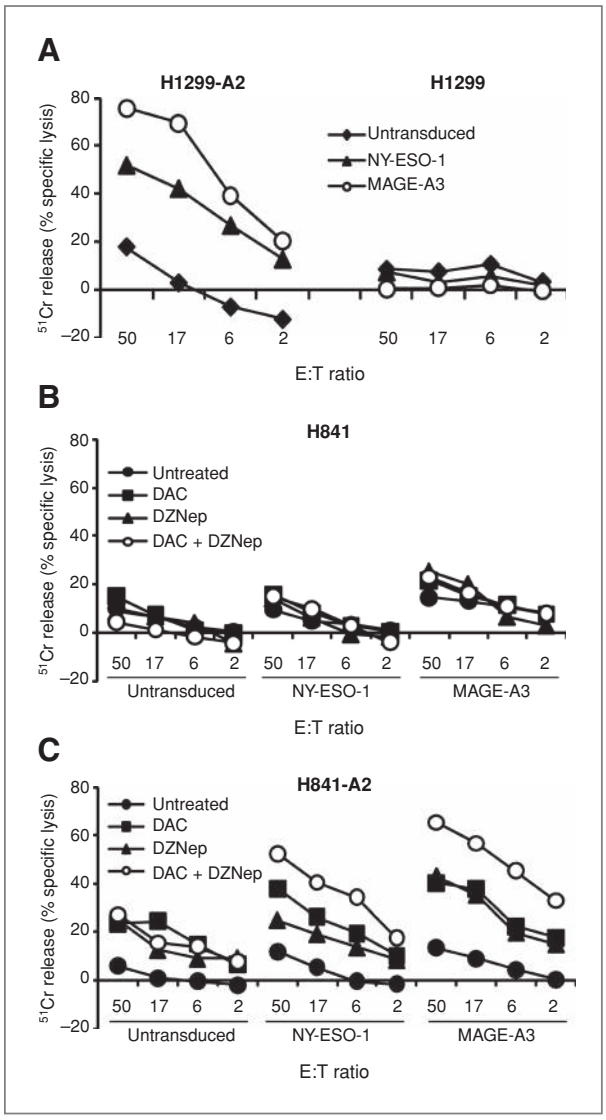

Figure 7. A, ^{51}Cr release assay depicting lysis of H1299 and H1299-A2 targets by NY-ESO-1 and MAGE-A3 TCR–transduced PBLs. Minimal lysis was observed against HLA-A2 negative cells. B and C, lysis of H841 and H842-A2 cells by NY-ESO-1 or MAGE-A3 or control vector–transduced PBLs following pretreatment of tumor targets with DAC, DZNep, or DAC–DZNep. Both NY-ESO-1 and MAGE-A3 effector cells mediated lysis of untreated H1299-A2 and H841-A2 targets following DAC, DZNep, or DAC–DZNep treatment. Pretreatment of tumor targets with DAC, DZNep, or DAC–DZNep markedly enhanced specific lysis mediated by NY-ESO-1 and MAGE-A3 effector cells. E:T, ratio of effector to target.

of H841-A2 cells treated with DAC exceeded that observed following treatment of target cells with DZNep for NY-ESO-1 effector cells, percent lysis following exposure of tumor targets to DZNep was comparable to that observed following treatment with DAC when tumor targets were cocultured with MAGE-A3 effector cells. Concurrent DAC–DZNep treatment of target cells markedly enhanced the percentage of specific lysis mediated by NY-ESO-1 or MAGE-A3 effector cells. The magnitude of lysis of DAC-, DZNep-, or DAC–DZNep-treated H841-A2 cells by MAGE-A3 effector cells exceeded that observed for NY-ESO-1 effector cells, possibly due to simultaneous upregulation of other *MAGE-A* genes such as *MAGE-A12* encoding HLA-A*0201-restricted epitopes recognized by the genetically engineered MAGE-A3 TCR (15). Specific lysis of H841-A2 cells by NY-ESO-1 and MAGE-A3 effector cells corresponded with mRNA copy numbers (Supplementary Table S6) and IFN-γ release observed in coculture assays.

Discussion

DNA methylation is the major epigenetic mechanism silencing CT-X genes in normal somatic cells (30, 31). Whereas CT-X gene expression can be induced in cancer cells by DNA-demethylating agents (10) or simultaneous knockdown of *DNMT1* and *DNMT3b* (32, 33), derepression of CT-X genes during malignant transformation cannot be attributed solely to global DNA demethylation. Transfected methylated *MAGE-A1* transgenes do not undergo promoter demethylation, and unmethylated *MAGE-A1* transgenes become methylated except for the 5′-region in cancer cells (34). Complex chromatin architecture including formation of double cruciform DNA (35) that potentially affects access of methyl-binding proteins, DNA methyltransferases, and transcription factors such as CTCF, BORIS, and SP1 (8, 32, 36) may contribute to coordinated repression/activation of CT-X genes within large inverted repeats (7).

In the present study, we sought to examine the feasibility of modulating histone lysine methylation as a strategy to enhance CT-X gene activation by DNA-demethylating agents under conditions potentially achievable in clinical settings (16). Our experiments showed that knockdown of *KMT6*, *KDM1*, and *KDM5B* significantly enhances DAC-mediated activation of *NY-ESO-1* and several *MAGE-A* genes in lung cancer cells. Whereas knockdown of *KMT6*, *KDM1*, and *KDM5B* coincided with decreased occupancy of these histone lysine methyltransferases and their respective marks within the *NY-ESO-1*, *MAGE-A1*, and *MAGE-A3* promoters, our data do not exclude the possibility that depletion of these histone modifiers facilitates CT-X gene activation via mechanisms independent of inhibition of methyltransferase activity (37).

Originally developed as an antiviral agent (38), DZNep has been shown to deplete KMT6, EED, and SUZ12 primarily via proteolytic mechanisms leading to growth arrest, differentiation, or apoptosis in cancer cells depending on histology and genotype (refs. 29, 39–42; Kemp and colleagues, unpublished data). Of particular interest, tumor-initiating cells appear exquisitely sensitive to DZNep, due to the critical role of polycomb proteins in maintenance of cancer stem cells (43). In addition to decreasing global H3K27Me3 levels, DZNep diminishes numerous other repressive and activation histone lysine methylation marks such as H3K9Me2 and H3K4Me3, respectively (44). DZNep reactivates genes silenced by polycomb mechanisms; however, despite the fact that DZNep exhibits mild DNA-demethylating effects, this agent is insufficient to derepress hypermethylated genes (44). Our analysis revealed that low-dose DZNep alone did not activate *NY-ESO-1*, *MAGE-A1*, or *MAGE-A3* in lung cancer cells, but significantly enhanced DAC-mediated induction of these

CT-X genes. Although our experiments suggested that enhancement of DAC-mediated CT-X gene induction by DZNep is attributable, in part, to depletion of KMT6, the precise mechanisms underlying this phenomenon have not been fully defined and are a focus of ongoing experiments.

Deciphering the mechanisms mediating derepression of CT-X genes in cancer cells may provide fundamental insights about malignant transformation and facilitate development of novel strategies for epigenetic therapy for cancer. Our observations that DZNep enhances DAC-mediated upregulation of NY-ESO-1 and MAGE-A family members, and markedly augments recognition and lysis of lung cancer cells by T cells specific for these CTAs, have direct translational implications about the development of gene-induction regimens for cancer immunotherapy. Our findings pertaining to the lack of CT-X gene induction in normal cells following DAC–DZNep exposure are consistent with our previously published data showing negligible activation of CT-X genes in SAECs or NHBE cells by DAC/DP (13, 14) or in normal tissues from lung cancer patients receiving these agents (16, 45). The fact that the magnitude of DAC–DZNep (as well as DAC/DP)-mediated CT-X gene induction is more pronounced in HBECs relative to SAECs, NHBE cells, or NHDFs, but less than in lung cancer cells with similar proliferation rates, suggests that global methylation changes associated with malignant transformation (18) contribute, in part, to the relative sensitivity of cancer cells to epigenetic treatment regimens. Although the mechanisms underlying this intriguing phenomenon remain elusive and are a focus of ongoing investigation, our data support further development of DZNep and other inhibitors of histone lysine methylation for cancer immunotherapy.

Disclosure of Potential Conflicts of Interest

No potential conflicts of interest were disclosed.

Acknowledgments

The authors thank Ms. Jan Pappas for assistance with the preparation of the manuscript.

The costs of publication of this article were defrayed in part by the payment of page charges. This article must therefore be hereby marked *advertisement* in accordance with 18 U.S.C. Section 1734 solely to indicate this fact.

Received July 7, 2010; revised April 7, 2011; accepted April 14, 2011; published OnlineFirst May 5, 2011.

References

1. Almeida LG, Sakabe NJ, deOliveira AR, Silva MCC, Mundstein AS, Cohen T, et al. CTdatabase: a knowledge-base of high-throughput and curated data on cancer-testis antigens. Nucleic Acids Res 2009;37:D816–19.
2. Caballero OL, Chen YT. Cancer/testis (CT) antigens: potential targets for immunotherapy. Cancer Sci 2009;100:2014–21.
3. Karbach J, Gnjatic S, Bender A, Neumann A, Weidmann E, Yuan J, et al. Tumor-reactive CD8+ T-cell responses after vaccination with NY-ESO-1 peptide, CpG 7909 and Montanide ISA-51: association with survival. Int J Cancer 2010;126:909–18.
4. Carrasco J, Van Pel A, Neyns B, Lethé B, Brasseur F, Renkvist N, et al. Vaccination of a melanoma patient with mature dendritic cells pulsed with MAGE-3 peptides triggers the activity of nonvaccine anti-tumor cells. J Immunol 2008;180:3585–93.
5. Robbins PF, Morgan RA, Feldman SA, Yang JC, Sherry RM, Dudley ME, et al. Tumor regression in patients with metastatic synovial cell sarcoma and melanoma using genetically engineered lymphocytes reactive with NY-ESO-1. J Clin Oncol 2011;29:917–24.
6. Stevenson BJ, Iseli C, Panji S, Zahn-Zabal M, Hide W, Old LJ, et al. Rapid evolution of cancer/testis genes on the X chromosome. BMC Genomics 2007;8:129.
7. Bredenbeck A, Hollstein VM, Trefzer U, Sterry W, Walden P, Losch FO. Coordinated expression of clustered cancer/testis genes encoded in a large inverted repeat DNA structure. Gene 2008;415:68–73.
8. Hong JA, Kang Y, Abdullaev Z, Flanagan PT, Pack SD, Fischette MR, et al. Reciprocal binding of CTCF and BORIS to the NY-ESO-1 promoter coincides with derepression of this cancer–testis gene in lung cancer cells. Cancer Res 2005;65:7763–74.
9. Vatolin S, Abdullaev Z, Pack SD, Flanagan PT, Custer M, Loukinov DI, et al. Conditional expression of the CTCF-paralogous transcriptional factor BORIS in normal cells results in demethylation and derepression of MAGE-A1 and reactivation of other cancer–testis genes. Cancer Res 2005;65:7751–62.
10. Schrump DS, Nguyen DM. Targeting the epigenome for the treatment and prevention of lung cancer. Semin Oncol 2005;32:488–502.
11. Stockert E, Jäger E, Chen YT, Scanlan MJ, Gout I, Karbach J, et al. A survey of the humoral immune response of cancer patients to a panel of human tumor antigens. J Exp Med 1998;187:1349–54.
12. Groeper C, Gambazzi F, Zajac P, Bubendorf L, Adamina M, Rosenthal R, et al. Cancer/testis antigen expression and specific cytotoxic T lymphocyte responses in non-small cell lung cancer. Int J Cancer 2007;120:337–43.
13. Weiser TS, Guo ZS, Ohnmacht GA, Parkhurst ML, Tong-On P, Marincola FM, et al. Sequential 5-Aza-2 deoxycytidine-depsipeptide FR901228 treatment induces apoptosis preferentially in cancer cells and facilitates their recognition by cytolytic T lymphocytes specific for NY-ESO-1. J Immunother 2001;24:151–61.
14. Wargo JA, Robbins PF, Li Y, Zhao Y, El-Gamil M, Caragacianu D, et al. Recognition of NY-ESO-1+ tumor cells by engineered lymphocytes is enhanced by improved vector design and epigenetic modulation of tumor antigen expression. Cancer Immunol Immunother 2009;58:383–94.
15. Chinnasamy N, Wargo JA, Yu Z, Rao M, Frankel TL, Riley JP, et al. A TCR targeting the HLA-A*0201-restricted epitope of MAGE-A3 recognizes multiple epitopes of the MAGE-A antigen superfamily in several types of cancer. J Immunol 2011;186:685–96.
16. Schrump DS, Fischette MR, Nguyen DM, Zhao M, Li X, Kunst TF, et al. Phase I study of decitabine-mediated gene expression in patients with cancers involving the lungs, esophagus, or pleura. Clin Cancer Res 2006;12:5777–85.
17. Guo ZS, Hong JA, Irvine KR, Chen GA, Spiess PJ, Liu Y, et al. *De novo* induction of a cancer/testis antigen by 5-aza-2′-deoxycytidine augments adoptive immunotherapy in a murine tumor model. Cancer Res 2006;66:1105–13.
18. Liu F, Killian JK, Yang M, Walker RL, Hong JA, Zhang M, et al. Epigenomic alterations and gene expression profiles in respiratory epithelia exposed to cigarette smoke condensate. Oncogene 2010;29:3650–64.
19. Xi S, Yang M, Tao Y, Xu H, Shan J, Inchauste S, et al. Cigarette smoke induces C/EBP-beta-mediated activation of miR-31 in normal human respiratory epithelia and lung cancer cells. PLoS One 2010;5:e13764.
20. Liu W, Cheng S, Asa SL, Ezzat S. The melanoma-associated antigen A3 mediates fibronectin-controlled cancer progression and metastasis. Cancer Res 2008;68:8104–12.
21. CpG Island Searcher [cited 2011 May 23]. Available from: http://cpgislands.usc.edu/
22. Hussain M, Rao M, Humphries AE, Hong JA, Liu F, Yang M, et al. Tobacco smoke induces polycomb-mediated repression of Dickkopf-1 in lung cancer cells. Cancer Res 2009;69:3570–8.
23. Zhao Y, Zheng Z, Robbins PF, Khong HT, Rosenberg SA, Morgan RA. Primary human lymphocytes transduced with NY-ESO-1

antigen-specific TCR genes recognize and kill diverse human tumor cell lines. J Immunol 2005;174:4415–23.
24. McGarvey KM, Fahrner JA, Greene E, Martens J, Jenuwein T, Baylin SB. Silenced tumor suppressor genes reactivated by DNA demethylation do not return to a fully euchromatic chromatin state. Cancer Res 2006;66:3541–9.
25. Wiencke JK, Zheng S, Morrison Z, Yeh RF. Differentially expressed genes are marked by histone 3 lysine 9 trimethylation in human cancer cells. Oncogene 2008;27:2412–21.
26. Shi Y, Lan F, Matson C, Mulligan P, Whetstine JR, Cole PA, et al. Histone demethylation mediated by the nuclear amine oxidase homolog LSD1. Cell 2004;119:941–53.
27. Xiang Y, Zhu Z, Han G, Ye X, Xu B, Peng Z, et al. JARID1B is a histone H3 lysine 4 demethylase up-regulated in prostate cancer. Proc Natl Acad Sci U S A 2007;104:19226–31.
28. Cao R, Wang L, Wang H, Xia L, Erdjument-Bromage H, Tempst P, et al. Role of histone H3 lysine 27 methylation in Polycomb-group silencing. Science 2002;298:1039–43.
29. Tan J, Yang X, Zhuang L, Jiang X, Chen W, Lee PL, et al. Pharmacologic disruption of Polycomb-repressive complex 2-mediated gene repression selectively induces apoptosis in cancer cells. Genes Dev 2007;21:1050–63.
30. De Smet C, Lurquin C, Lethe B, Martelange V, Boon T. DNA methylation is the primary silencing mechanism for a set of germ line- and tumor-specific genes with a CpG-rich promoter. Mol Cell Biol 1999;19:7327–35.
31. Link PA, Gangisetty O, James SR, Woloszynska-Read A, Tachibana M, Shinkai Y, et al. Distinct roles for histone methyltransferases G9a and GLP in cancer germ-line antigen gene regulation in human cancer cells and murine embryonic stem cells. Mol Cancer Res 2009;7:851–62.
32. Kang Y, Hong JA, Chen GA, Nguyen DM, Schrump DS. Dynamic transcriptional regulatory complexes including BORIS, CTCF and Sp1 modulate NY-ESO-1 expression in lung cancer cells. Oncogene 2007;26:4394–403.
33. James SR, Link PA, Karpf AR. Epigenetic regulation of X-linked cancer/germline antigen genes by DNMT1 and DNMT3b. Oncogene 2006;25:6975–85.
34. De Smet C, Loriot A, Boon T. Promoter-dependent mechanism leading to selective hypomethylation within the 5′ region of gene MAGE-A1 in tumor cells. Mol Cell Biol 2004;24:4781–90.
35. Losch FO, Bredenbeck A, Hollstein VM, Walden P, Wrede P. Evidence for a large double-cruciform DNA structure on the X chromosome of human and chimpanzee. Hum Genet 2007;122:337–43.
36. Wischnewski F, Friese O, Pantel K, Schwarzenbach H. Methyl-CpG binding domain proteins and their involvement in the regulation of the MAGE-A1, MAGE-A2, MAGE-A3, and MAGE-A12 gene promoters. Mol Cancer Res 2007;5:749–59.
37. Yang Z, Jiang J, Stewart DM, Qi S, Yamane K, Li J, et al. AOF1 is a histone H3K4 demethylase possessing demethylase activity-independent repression function. Cell Res 2010;20:276–87.
38. Mayers DL, Mikovits JA, Joshi B, Hewlett IK, Estrada JS, Wolfe AD, et al. Anti-human immunodeficiency virus 1 (HIV-1. activities of 3-deazaadenosine analogs: increased potency against 3′-azido-3′-deoxythymidine-resistant HIV-1 strains. Proc Natl Acad Sci U S A 1995;92:215–19.
39. Puppe J, Drost R, Liu X, Joosse SA, Evers B, Cornelissen-Steijger P, et al. BRCA1-deficient mammary tumor cells are dependent on EZH2 expression and sensitive to Polycomb Repressive Complex 2-inhibitor 3-deazaneplanocin A. Breast Cancer Res 2009;11:R63.
40. Fiskus W, Wang Y, Sreekumar A, Buckley KM, Shi H, Jillella A, et al. Combined epigenetic therapy with the histone methyltransferase EZH2 inhibitor 3-deazaneplanocin A and the histone deacetylase inhibitor panobinostat against human AML cells. Blood 2009;114:2733–43.
41. Musch T, Oz Y, Lyko F, Breiling A. Nucleoside drugs induce cellular differentiation by caspase-dependent degradation of stem cell factors. PLoS One 2010;5:e10726.
42. Hayden A, Johnson PW, Packham G, Crabb SJ. *S*-adenosylhomocysteine hydrolase inhibition by 3-deazaneplanocin A analogues induces anti-cancer effects in breast cancer cell lines and synergy with both histone deacetylase and HER2 inhibition. Breast Cancer Res Treat 2011;127:109–19.
43. Suvà ML, Riggi N, Janiszewska M, Radovanovic I, Provero P, Stehle JC, et al. EZH2 is essential for glioblastoma cancer stem cell maintenance. Cancer Res 2009;69:9211–18.
44. Miranda TB, Cortez CC, Yoo CB, Liang G, Abe M, Kelly TK, et al. DZNep is a global histone methylation inhibitor that reactivates developmental genes not silenced by DNA methylation. Mol Cancer Ther 2009;8:1579–88.
45. Schrump DS, Fischette MR, Nguyen DM, Zhao M, Li X, Kunst TF, et al. Clinical and molecular responses in lung cancer patients receiving romidepsin. Clin Cancer Res 2008;14:188–98.